Nanoscale

Accepted Manuscript

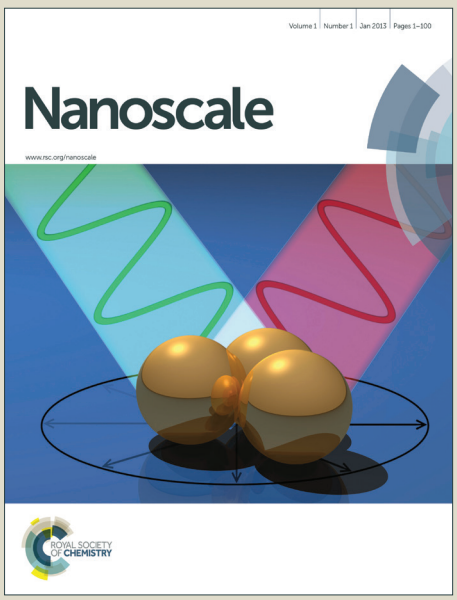

ROYAL SOCIETY OF CHEMISTRY

www.rsc.org/nanoscale

Strong Negative Nanocatalysis: Oxygen Reduction and Hydrogen Evolution at Very Small (2 nm) Gold Nanoparticles

Ying Wang[a], Eduardo Laborda[b], Kristina Tschulik[a], Christine Damm[c], Angela Molina[b], Richard G. Compton*[,a]

[a] *Department of Chemistry, Physical and Theoretical Chemistry Laboratory, Oxford University, South Parks Road, Oxford OX1 3QZ, United Kingdom*

[b] *Department of Physical Chemistry, Regional Campus of Excellence "Campus Mare Nostrum", Universidad de Murcia, Murcia, Spain*

[c] *IFW Dresden, Institute for Metallic Materials, P.O. Box 270016,D-01171 Dresden, Germany*

To be submitted as a Communication to: Nanoscale

* Corresponding author

Email: richard.compton@chem.ox.ac.uk

Tel:+44 (0) 1865 275 957

Fax:+44 (0) 1865 275 410

Abstract

The electron transfer kinetics associated with both the reduction of oxygen and of protons to form hydrogen at gold nanoparticles are shown to display strong retardation when studied at citrate capped ultra small (2 nm) gold nanoparticles. Negative nanocatalysis in the hydrogen evolution reaction (HER) is reported for the first time.

To sustainably account for the worldwide increasing consumption of energy, a mixture of renewable and clean technologies has to be established.[1–9] Many of today's green energy approaches, such as photocatalytic water splitting and the subsequent use of the produced hydrogen in fuel cells, include either the oxygen reduction reaction (ORR)[1–5] or the hydrogen evolution reaction (HER)[1–5] or a combination of both. Both these reactions have sluggish kinetics in the absence of a suitable catalyst. Enormous efforts on finding novel and better catalysts for both these reactions have been undertaken during the past decades and nanoparticular materials were found to be one of the most promising to reduce the total amount of the typically used noble metals and to thus reduce the costs. This is possible as nanoparticles provide a much higher surface area to volume ratio than bulk material.[10] Thus, the catalysis of the surface-sensitive ORR and HER requires for smaller amounts of the noble metal, allowing a decrease of production costs. This is true even more so the smaller the nanoparticle.[11] However, as lengths scales are reduced to the nm-region in addition to this purely geometric aspect, other material properties change and they may change drastically.[12] To name but a few of these nano-effects, changes in the electronic structure,[13,14] exposure of crystal facets[13,14] or surface curvature[15] can be mentioned. While identifying the reason for this is simple, the inherent overlap of a strongly improved mass transport and often comparably small changes in the catalytic activity of the material, delineating the two is not. This delineation, however, is of upmost importance, as only after having separated the two influences, nanoparticulate materials can be designed so as to optimize both mass transport enhancement and catalytic

activity at the same time.

Our group has recently developed a generic electrochemical strategy[16–18] for the rigorous evaluation of the electrocatalytic properties of metallic nanoparticles. This is based on the analysis of the experimental electrochemical response of a macroelectrode decorated with nanoparticles. In contrast to previous semi-empirical approaches, we take into account *both* the changes in the mass transport conditions *and* in the electron transfer kinetics as a result of the nanoparticle modification. Decoupling mass transport effects is essential for identifying authentic catalysis since electrode modification inevitably alters the transport conditions.[19,20] Proof on concept was realised for investigating the kinetics of the oxygen reduction reaction (ORR) on gold nanoparticles between 5 - 40 nm in diameter in oxygen-saturated 0.5 M sulfuric acid.[17,18]

Making use of this strategy, here we consider the electrocatalytic activity of 2 nm citrate capped gold nanoparticles (Au-NPs) towards both the ORR and the HER. As indicated above, this has a great practical significance for the rational development of efficient electrocatalysts and it is also of fundamental interest given that such small particles lie at the frontier between isolated molecules and bulk materials and so between classical physics and quantum mechanics. The main steps followed for the characterization of the Au NP catalytic activity are summarized in Figure. 1.

First, we discuss the details of the glassy carbon electrode (GCE) modification and the determination of the NP coverage, which are common to the studies of both the ORR and

the HER reactions. Citrate capped gold nanoparticles are employed in this study given that citrate is one of the most widely-employed capping agents. Citrate is also relatively weakly bound to the gold nanoparticle surface and being a short-chain molecule it allows the access of the electroactive species to the surface active sites. Further electron tunneling is less hindered than with larger and/or more strongly-adsorbed capping agents.[16,21,22] TEM analysis (displayed in Figure.2.a) shows that the commecially purchased citrate capped gold nanoparticles are spherical in shape and the diameter is 1.9 ± 0.8 nm. A GCE is chosen as substrate on which to examine nanoparticle catalytic behaviour given that GCE shows poor electrocatalytic ability towards ORR and HER such that it offers a clean potential window where the ORR and HER responses on Au NPs can be studied without significant interference of the substrate. To modify the GCE, it is immersed in a Au NP solution (0.38 μM gold nanoparticles in 0.1 M $NaClO_4$) where nanoparticles adsorb on the surface and modify the electrode. To ensure that the deposited nanoparticles are evenly distributed on the electrode surface, electrophoresis is employed to modify the glassy carbon surface with gold nanoparticles. This method has been successfully employed previously by several authors, including ourselves, to produce homogenous distribution of particles, as confirmed by (field emission) scanning electron microscopy and transmission electron microscopy.[18,23–26] In other techniques such as drop-casting the particles were observed to concentrate in a small region of the GCE surface during the drying process, which can also promote particle aggregation.[27,28] This is important to be avoided in order to assure accurate results given that the theoretical modeling employed here assumes that the

NPs resemble an array of uniform and evenly-distributed nanoelectrodes.[16,29]

The sticking of citrate-capped Au NPs onto GCE under open circuit conditions have been found to be very slow thus leading to very low coverage (less than 1%, beyond the detection limit of anodic stripping coulometry in HCl, see below) even after long modification times.[18] Following the methodology employed successfully in a previous paper,[18] the application of a positive potential for the electrode modification was examined in order to enhance the flux of the negatively-charged citrate-capped NPs towards the GCE and achieve higher coverage. An Electrophoretic potential of +0.1 V (vs. SCE) was applied in order to prevent the nanoparticle electro-oxidation. All the experiments are carried out with fresh commercial nanoparticle solutions subject to 5 min sonication before each GCE modification in order to prevent NP aggregation and settling, which result in lower nanoparticle sticking.

Knowledge of nanoparticle coverage is the key factor allowing rigorous quantitative studies. First, the highest NP coverages which can be studied are set by the theoretical model where the nanoparticles are supposed to be of uniform size and evenly distributed on the GCE surface. For instance, a 15% coverage means that *even if* the distribution of the particles was perfectly homogeneous the average interparticle distance would be less than 6 nm. The formation of aggregates and porous structures cannot be discarded under such conditions which is not accounted for in our simulations. Also, when modifying surfaces with nanosized materials the ultimate goal is to use as little of the (typically expensive noble-metal based) material as possible and to avoid agglomeration of the nanoparticles, so as to avoid losing positive nano-effects

towards more bulk-like behavior. Thus, a homogeneous distribution of reasonably-spaced individual particles is envisaged for both practical engineering aspects and theoretical analysis purposes. Secondly, figure 3 shows the ORR voltammograms on bare GCE (solid line) and Au-NPs/GCE with 3 % (dashed line) and 7 % (dotted line) NP coverage in an oxygen-saturated 0.5 M sulfuric acid at 298 K and 750 mVs^{-1}. From the figure it can be inferred that there is a very significant contribution from the substrate to the ORR signal (that is, from ORR on bare GC regions) for 3 % coverage such that the electrochemical response is less informative about the ORR kinetics on Au NPs.

Considering all the above factors, a modification time of 60 min was found to be adequate given that it yields an appropriate coverage value of *ca.* 6 % - 8% such that the recorded signal reflects quantitatively the kinetics on Au NPs while keeping the experimental time acceptably short.

The number of nanoparticles deposited on the glassy carbon electrode was estimated from the anodic stripping charge of the particles in 0.1 M hydrochloric acid by consecutive linear sweep voltammetries at 50 mVs^{-1}, which has been successfully employed in previous studies.[16–18,30] Finot[31] and Kolics[32] reported that the electro-oxidation products of bulk gold in hydrochloric acid are the $AuCl_4^-$ and $AuCl_2^-$ complexes. More recently,[33] this conclusion was extended to the case of gold nanoparticles such that the NP stripping involves 1.9 ± 0.1 electrons transferred *per* gold atom. Given that TEM images prove the nanoparticles to be of spherical shape, the number of nanoparticles (N) can be immediately related to the stripping

charge (Q) provided that the average radius of the particles (r) is known:

$$N = Q \times \frac{M_{Au}}{1.9\, e\, \frac{4}{3}\pi r^3\, \rho_{Au}\, N_A} \tag{1}$$

where e is the elementary charge, ρ_{Au} the density of gold, M_{Au} its molar mass and N_A the Avogadro constant. Once number of nanoparticles is obtained, the NP coverage is defined as:

$$\Theta = 100 \times \frac{\pi r^2 N}{A} \tag{2}$$

Figure 2.b shows the anodic stripping voltammogram at a Au-NP/GCE in 0.1 M HCl at 298 K and 50 mVs^{-1}. A typical stripping peak of citrate-capped gold nanoparticles appears at +0.96 V (*vs.* SCE).[33]

Next, we report the Au NP electrocatalytic activity towards ORR. All the electrochemistry measurements of ORR on Au-NPs/GCE were carried out in oxygen saturated 0.5 M sulfuric acid at 298 K. Figure 4 shows the background-subtracted experimental voltamogramms for ORR in an oxygen-saturated 0.5 M sulfuric acid solution ($T = 298$ K, a: $v = 750$ mVs^{-1}, b: $v = 100$ mVs^{-1}) on bare GCE (dashed line) and on Au-NP/GCE (solid line). The NP coverages of Au-NP/GCE are *ca.* 7 % based on the anodic stripping charge in HCl measured just after the ORR experiments. The cyclic voltammetry study was performed in the scan rate range 100-750 mVs^{-1}. The experimental voltammograms show that the electrocatalytic performance of the nanoparticle-modified electrode is higher than bare GCE. To determine how this performance

compares with that of bulk gold in order to detect possible changes in the ORR kinetics as a result of nanoeffects, we make use of a simulation program developed in our group, which enables the rigorous simulation of cyclic voltammetry experiments on nanoparticle-modified electrodes, taking into account the remarkable differences between the mass transport at a macroelectrode and at an array of particles acting as nanoelectrodes. This program models the modified-electrode surface as an array of uniform sized and evenly distributed spherical nanoelectrodes resting on a substrate.[16,29] For the electron transfer kinetics at the NP surface, the Butler-Volmer formalism is employed[34] and the concentrations of the different species in solution are subject to mass transport by diffusion and the chemical transformations established by the reaction scheme (see Eq.3-6). The resulting diffusive-kinetic differential equation system is solved by finite-difference methods for cyclic voltammetry conditions. The fitting of the experimental voltammograms enables the quantitative characterization of the electrochemical kinetics at the nanoparticles taking into account the interplay between the NP diffusion domains. First, the ORR reaction mechanism needs to be defined. This has been extensively studied in the past[35–40] such that the mechanism on gold in acid media is generally accepted as a two-electron, two-proton transfer process with hydrogen peroxide as the final product ((3)-(6)) where the first electron transfer step is rate determining:

$$O_2 + e^- \overset{k_{0,1},E_1^0,\alpha_1}{\rightleftharpoons} O_2^{-\cdot} \quad (slow) \tag{3}$$

$$O_2^{-\cdot} + H^+ \overset{K_{eq1},k_{f1}}{\rightleftharpoons} HO_2^{\cdot} \tag{4}$$

$$HO_2^{\cdot} + e^- \overset{E_2^0 \gg E_1^0}{\longrightarrow} HO_2^- \quad (fast) \tag{5}$$

$$HO_2^- + H^+ \overset{K_{eq2}, k_{f2}}{\rightleftharpoons} H_2O_2 \tag{6}$$

where $k_{0,i}$ is the electron transfer rate constant, α_i the transfer coefficient, E_i^0 the formal potential, K_{eqi} the equilibrium constant and k_{fi} the forward rate constant of step i. Under the experimental conditions of this study, the diffusion coefficient and concentration of oxygen in 0.5 M sulfuric acid are $(1.26 \pm 0.03) \times 10^{-5}$ cm^2 s^{-1} and 1.43 ± 0.02 mM, respectively.[17,40]

By implementing the reaction mechanism given by (3)-(6) in the home-written simulation program, the cyclic voltammetry response expected if the ORR kinetics on the Au NPs was the same as on bulk gold was simulated (open circle in Figure 4). The coverage of Au NPs were ca. 7 %, these were determined from anodic stripping in HCl after each experiment. Thus, the ORR kinetic parameters obtained on bulk gold in previous studies[17] were employed (see Table 1), along with the NP coverage and the average NP size extracted from the TEM images (1.9 nm). By comparing the experimental (solid line) and simulated (open circle) results one can observe a clear increase of the overpotential (*ca.* −330 mV) and decrease of the peak current (10 %) when moving from bulk gold to Au NPs. This reveals the fact that the ORR kinetics slows down on 1.9 nm gold nanoparticles compared to bulk gold; a significant *negative* effect is observed. Note that this negative effect is not found for ORR under the same conditions on gold nanoparticles of sizes between 5 nm and 40 nm.[17,18]

The negative nanoeffect shown in Fig.4 is further proved by quantitative studies using

Tafel analysis and fitting of the experimental voltammograms with the home-written simulation program. Thus, satisfactory fittings (open triangle) of the experimental curves from 100 mVs^{-1} (Fig. 4.b) to 750 mVs^{-1} (Fig. 4.a) are obtained with a transfer coefficient (α_1) of 0.37 ± 0.01 and a standard electrochemical rate constant of (1.6 ± 0.3) × 10^{-3} $cm\,s^{-1}$. Note that the former is in very good agreement with the transfer coefficient value evaluated from the Tafel plot (0.36) (inset in Fig. 4.a).

As summarized in Table 1, the ORR kinetics on 1.9 nm Au NPs is significantly slower than on gold macroelectrodes. This also means that the 1.9 nm Au NPs are poorer catalysts for the ORR in this media than the larger particles (5-40 nm) previously investigated, where the ORR kinetics was found to be very similar to that at macroelectrodes.[17,18]

Next, we study the HER kinetics at gold nanoparticles to see if negative catalysis also exists for that reaction. We first quantified the kinetic behaviour at a gold macroelectrode using cyclic voltammograms obtained in nitrogen-saturated 0.5 M sulfuric acid between 100 and 750 mVs^{-1} (solid line in Figures 5.a and 5.b). The electron transfer kinetics are quantified by Tafel analysis and fitting of experimental cyclic voltammograms from 100 mVs^{-1} to 750 mVs^{-1} with the commercial simulation software DigiSim. In order to apply DigiSim to quantify the electron transfer kinetics, the mechanism of HER need first to be considered. It is widely accepted as the following steps:[1,41]

$$\mathrm{H^+} + e^- \overset{k_{0,3},E_3^0,\alpha_3}{\longrightarrow} \mathrm{H_{ad}} \quad (slow) \tag{7}$$

$$\mathrm{H}_{ad} + \mathrm{H^+} + e^- \longrightarrow \mathrm{H_2}\,(g) \quad (fast) \tag{8}$$

where, $k_{0,i}$ is the electron transfer rate constant, α_i the transfer coefficient and E_i^0 the formal potential of step i.

The first step where protons are electro-reduced to adsorbed atomic hydrogen is thought to be rate determining.[1] Subsequently, adsorbed atomic hydrogen combines with a proton and is further reduced to molecular hydrogen.

As shown in Figures 5.a and 5.b, a satisfactory fitting of the experimental (solid line) and simulated (open circle) voltamograms are obtained in the whole range of scan rates with a standard electron transfer rate constant ($k_{0,3}$) of 6.4 $\times$ 10^{-7} cm s^{-1} and a transfer coefficient value of 0.46$\pm$ 0.01. The latter compares well with the α_3 value (0.47) obtained from the Tafel plot (inset in Figure 5.a) and the literature.[1,21]

Next, cyclic voltammetry experiments were performed with Au NP-modified electrodes. Figures 5.c (750 mVs^{-1}) and 5.d (100 mVs^{-1}) show the comparison of the HER experimental signals in nitrogen-saturated 0.5 M sulfuric acid solution at 298 K on Au-NP/GCE (solid line) and bare GCE (dashed line). According to the gold anodic stripping charge in HCl, the NP coverage is 7% and 7.5% for 750 mVs^{-1} and 100 mVs^{-1}, respectively. The voltammograms show in that the presence of Au NPs on the GCE surface catalyzes the HER reaction. However, when comparing the experimental signal (solid line) with the home-written simulations run with the kinetic parameters above-obtained for gold macroelectrodes (open circle) of the same coverage, a lower catalytic activity by the Au NPs with respect to bulk gold can be inferred.

In order to quantify these changes, the $k_{0,3}$ value and the transfer coefficient value were

obtained from the fitting of the current-potential curves with the home-written simulation program from 100 mVs^{-1} to 750 mVs^{-1}. The best-fit curves (open triangle) corresponds to the values $k_{0,3}$ =(9.0 ± 0.1) × 10^{-8} $cm\,s^{-1}$ and α_3 =0.53 ± 0.01, respectively. The latter fully agrees with the α_3 value obtained in the Tafel analysis (0.53, see inset in Figure 5.c) and $k_{0,3}$ at Au NPs is significantly smaller than the value obtained at gold macroelectrodes (see Table 1).

The above results clearly reveal a slowing down of the electrochemical kinetics of both ORR and HER on 1.9 nm citrate capped gold nanoparticles in strong acid media. In the case of ORR no kinetic changes on larger gold nanoparticles supported on a glassy-carbon electrode (5 nm and 40 nm).[17,18] This enables us to discard support-only effects. Also, mass transport effects can be disregarded given that the theoretical model describes it rigorously. Therefore, the behavior reported here is particle size-related and it seems to be apparent only for NP diameters below 5 nm.

The above conclusion is compatible with other claims of a loss of activity of gold and platinum NPs towards oxygen reduction and carbon monoxide oxidation when the particles are smaller than 2-3 nm,[42] which was rationalized in terms of the oxygen binding energy at low coordinate sites that are more abundant at small particles. Nevertheless, to pinpoint the origins behind this behaviour is not straightforward considering the interplay of a number of structural (facets, defects,...) and electronic (which can be significant for such small particles) effects associated with nanoparticulate materials.[43] The observation of the negative electrocatalytic

effect for the HER at small nanoparticles is entirely novel.

In summary, for ORR, the standard electron transfer rate constant decreases from 0.3 $\mathrm{cm\,s^{-1}}$ [17] in the macro gold electrode to $(1.6 \pm 0.3) \times 10^{-3}$ $\mathrm{cm\,s^{-1}}$ on the 1.9 nm Au NPs while the transfer coefficient changes from 0.45 [17] in the macroscale to 0.37 ± 0.01 at the nanoparticles under study. The values obtained for 1.9 nm Au NPs are also smaller than those reported for larger glassy carbon-supported gold nanoparticles (5-40 nm), which reflects a clear slowing down of the ORR. A similar behaviour is manifested in HER with the standard electron transfer rate constant reducing from 6.4×10^{-7} $\mathrm{cm\,s^{-1}}$ at bulk gold to $(9.0 \pm 0.1) \times 10^{-8}$ $\mathrm{cm\,s^{-1}}$ on the Au NPs, and the transfer coefficient changing from 0.46 ± 0.01 to 0.53 ± 0.01 from the macro-scale to the nano-scale. Therefore, the results obtained clearly suggest negative electrocatalytic nanoeffects by the 1.9 nm citrate capped gold nanoparticles for both the oxygen reduction and hydrogen evolution reactions in sulfuric acid medium.

Experimental Section

Chemical reagents

Sulfuric acid (H_2SO_4, Fisher, >95%), hydrochloric acid (Sigma-Aldrich, >37%) and citrate-capped 1.9 nm gold nanoparticles (Nanopartz; Zeta potential = −30 mV) were all used without further purification. All the solutions were prepared using deionised water with resistivity of 18.2 MΩ cm (25 °C).

Instrumental

A three-electrode set-up with an Autolab PGStat 20 computer-controlled potentiostat (Eco-Chemie, Utrecht, Netherlands) were used for all the electrochemical measurements. A platinum wire was used as the counter electrode and a saturated calomel electrode (SCE, Radiometer, Copenhagen) as the reference electrode.

A bare or modified glassy carbon electrode (GCE, 3 mm diameter, BAS, Technical, UK) or a bare gold electrode (2mm diameter, BAS, Technical, UK) were employed as working electrodes. Glassy carbon electrode was polished using 3.0, 1.0 and 0.1 μm diamond spray (Kenet, Kent,UK) and gold electrode was polished with a decreasing size of 1.0, 0.3, 0.05 μm alumina lapping compounds (Bucher, Germany). All of them were sonicated in an ultrasound bath prior to use.

Transmission electron microscopy (TEM) images were obtained on FEI TECNAI T20 (200 kV/LaB6-filament/EDX-Oxford-detector). Both facetting of individual and possible agglomeration of multiple nanoparticles can be identified with diffraction contrast.

Acknowledgments

EL thanks the funding received from the European Union Seventh Framework Programme-Marie Curie COFUND (FP7/2007-2013) under the U-IMPACT action (Grant Agreement 267143). K.T. was supported by a Marie Curie Intra European Fellowship (Grant Agreement no. 327706) within the 7th European Community Framework Programme.

Table 1: Electron transfer kinetics of the oxygen reduction and hydrogen evolution reactions at gold macroelectrodes and at 1.9 nm citrate-capped Au-NPs at 298 K in 0.5 M sulfuric acid solution. The values reported correspond to the best fit of the cyclic voltammograms obtained at different scan rates between 100 and 750 $\mathrm{mV\,s^{-1}}$.

	ORR		HER	
	Au macroelectrode	Au-NPs	Au macroelectrode	Au-NPs
α	0.45[17,18]	0.37 ± 0.01	0.46± 0.01	0.53 ± 0.01
k_0 ($\mathrm{cm\,s^{-1}}$)	0.3[17,18]	$(1.6 \pm 0.3) \times 10^{-3}$	$(6.4\pm 0.6) \times 10^{-7}$	$(9.0 \pm 0.1) \times 10^{-8}$

Figure 1: Strategy applied in this work for the quantitative kinetic studies of the ORR and HER kinetics on 2 nm Au-NPs/GCE.

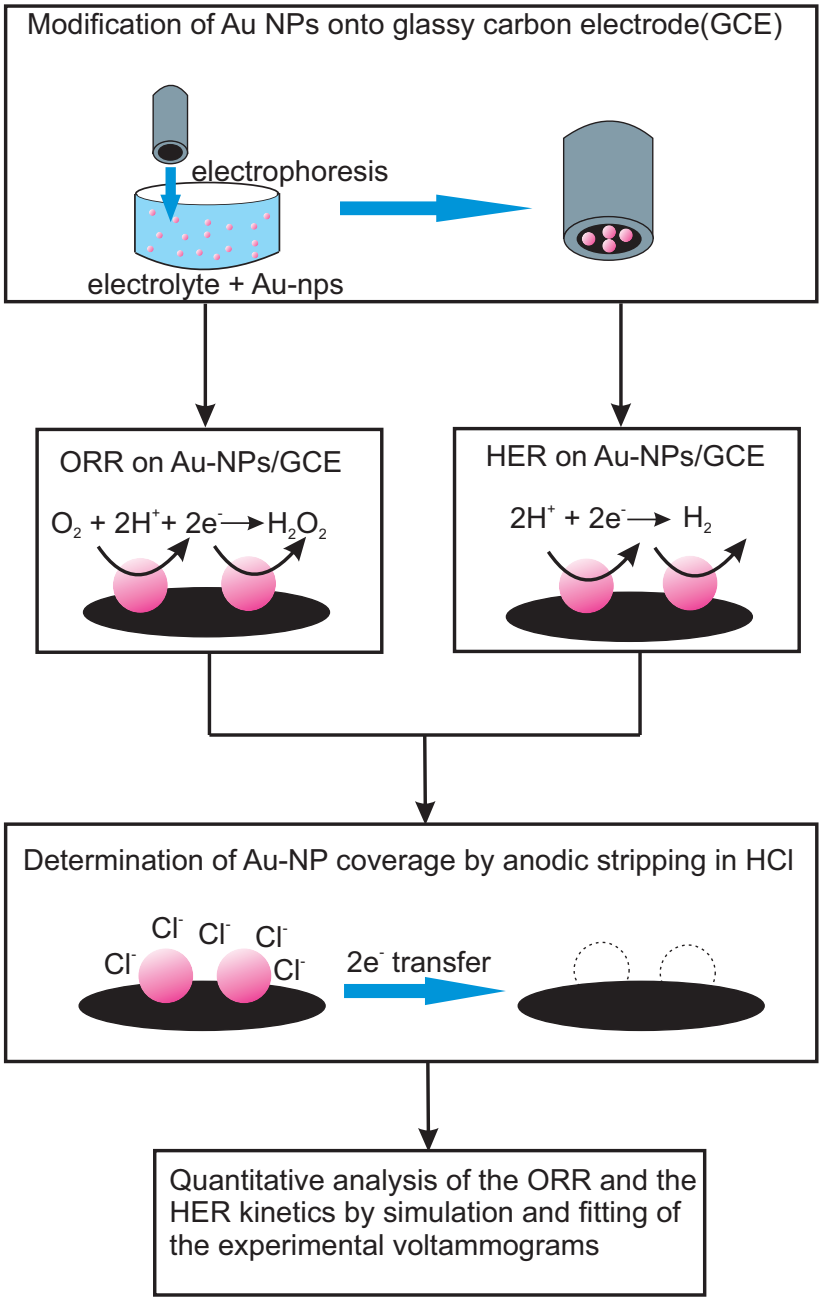

Figure 2: **(a)** TEM image of the citrate-capped gold nanoparticles investigated. **(b)** Anodic stripping of citrate capped gold nanoparticles from a modified glassy carbon electrode in 0.1 M HCl at 50 mVs^{-1}. $T = 298$ K.

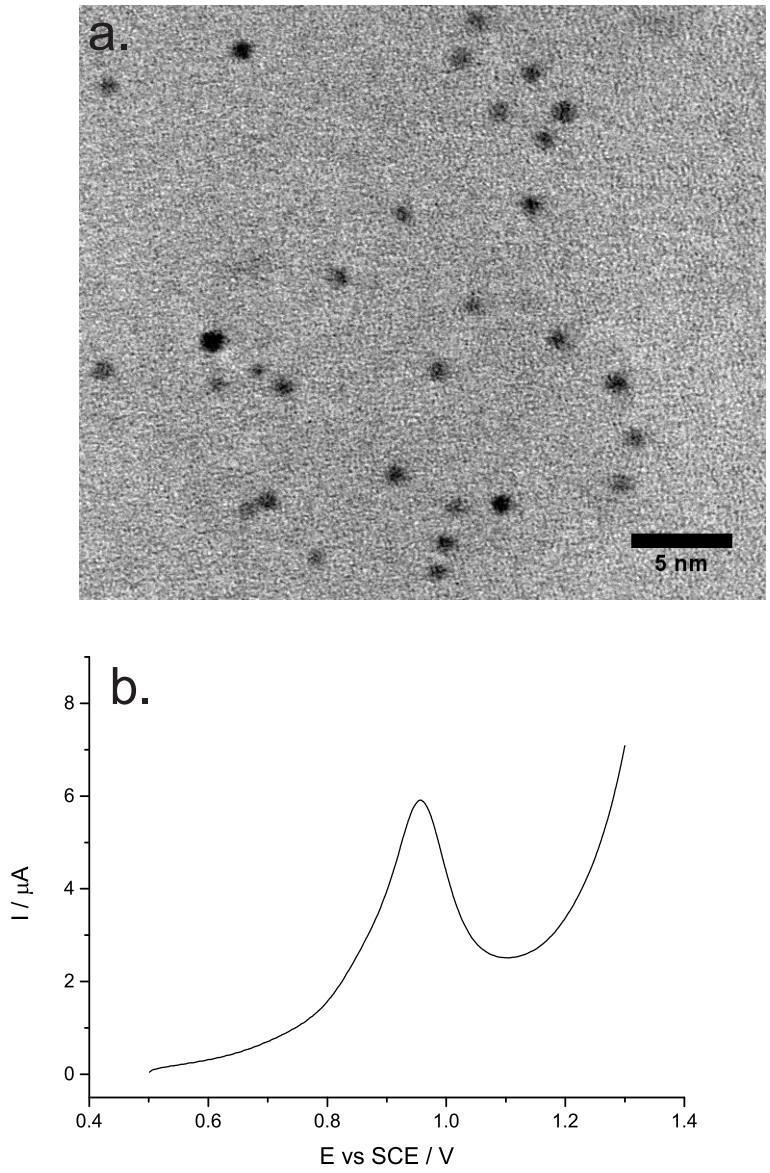

Figure 3: Experimental voltammograms for oxygen reduction reaction on a bare glassy carbon electrode (solid line), Au-NPs/GCE with 3 % (dashed line) and 7 % (dotted line) coverages at 298 K, 750 mVs^{-1}.

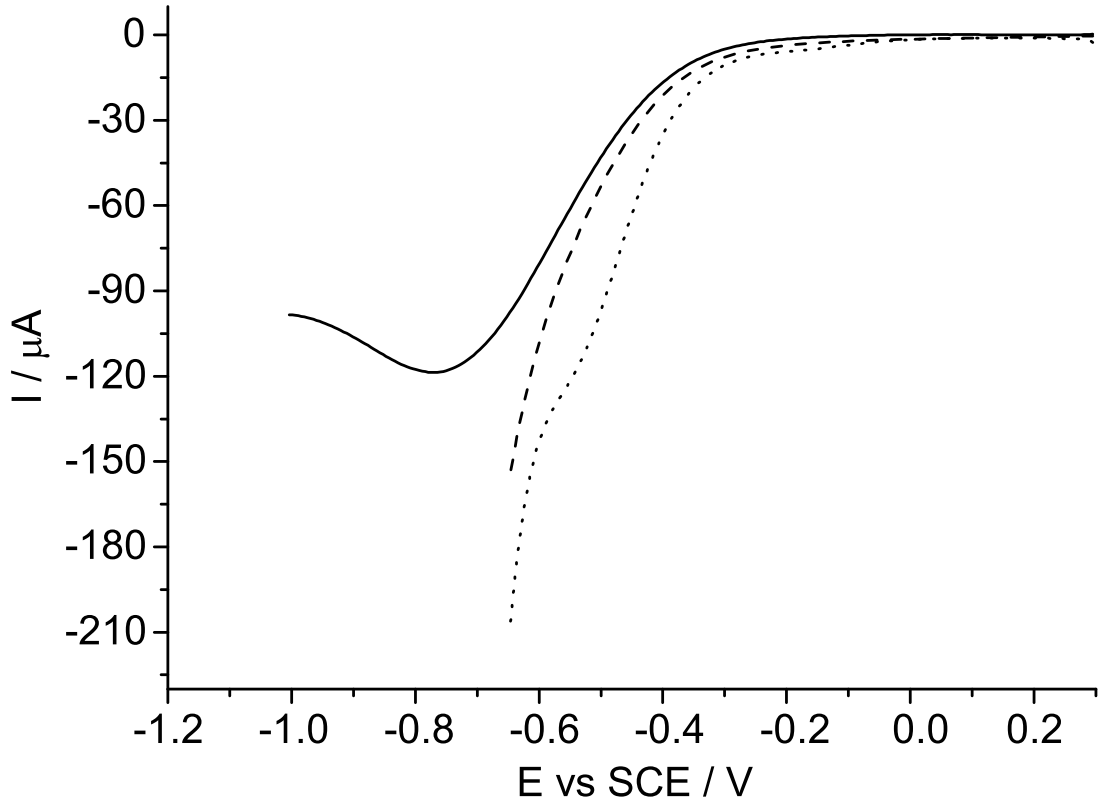

Figure 4: Comparison of experimental background-subtracted voltamogramms on bare glassy carbon electrode (dashed line), 1.9 nm Au-NP/GCE (solid line) and simulated voltammograms with the kinetics experimentally obtained for gold macro electrode (open circle) and for gold nanoparticles (open triangle) in oxygen saturated 0.5 M sulfuric acid at 750 and 100 mVs^{-1}. $T = 298$ K.

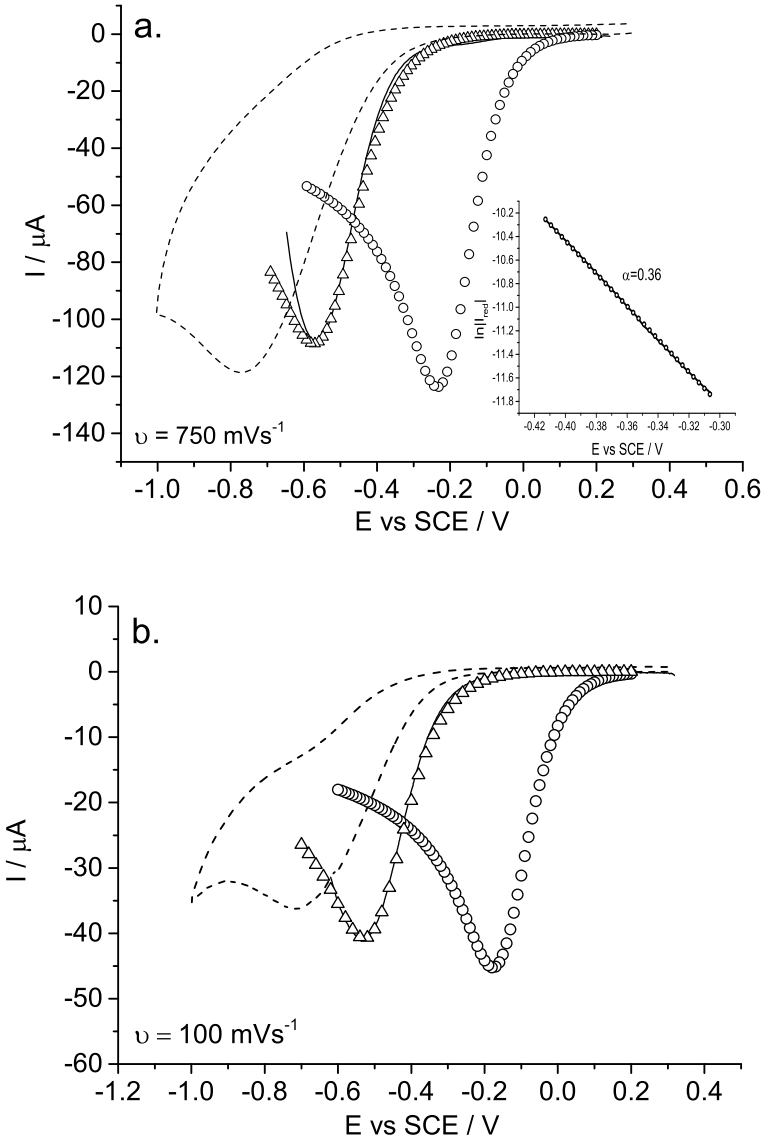

Figure 5: Experimental current-potential curves corresponding to the hydrogen evolution in nitrogen saturated 0.5 M sulfuric acid solution at 750 and 100 mVs^{-1} on a: **(a, b)** macro gold electrode (solid line); **(c, d)** citrate-capped 1.9 nm Au-NP/GCE (solid line) and bare GCE (dashed line). Simulated current-potential curves with the kinetics obtained experimentally for gold macro-electrodes (open circle) and for gold nanoparticles (open triangle). Diffusion coefficient of H^+: 8.8×10^{-5} $cm^2 \cdot s^{-1}$.[44] Insets: Tafel analyses. $T = 298$ K.

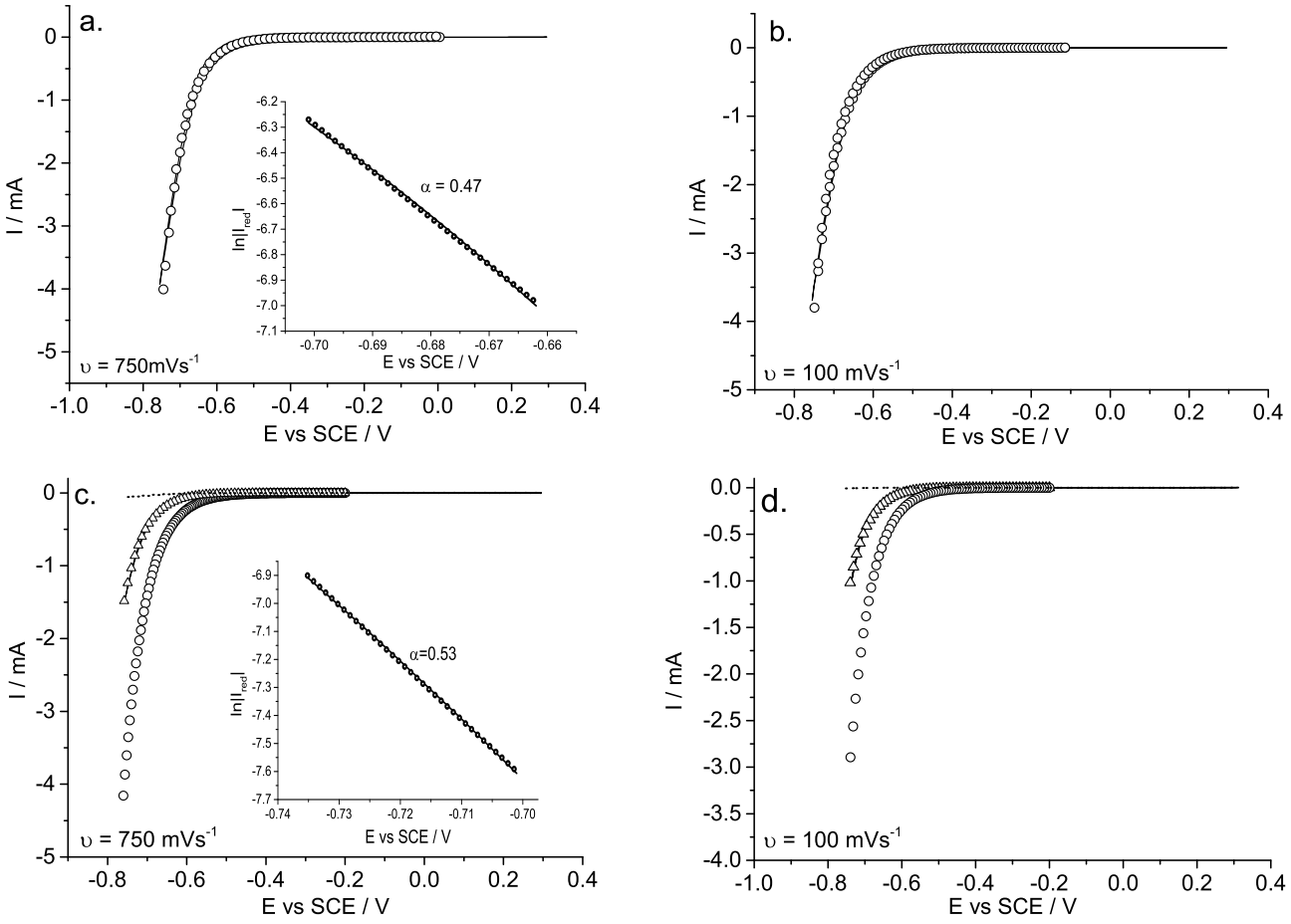

References

[1] O. Pecina and W. Schmickler, *Chemical Physics*, 1998, **228**, 265–277.

[2] W. Sheng, H. A. Gasteiger and Y. Shao-Horn, *Journal of The Electrochemical Society*, 2010, **157**, B1529–B1536.

[3] R. Michalsky, Y.-J. Zhang and A. A. Peterson, *ACS Catalysis*, 2014, **4**, 1274–1278.

[4] W. Sheng, M. Myint, J. G. Chen and Y. Yan, *Energy & Environmental Science*, 2013, **6**, 1509–1512.

[5] P. Millet, N. Mbemba, S. Grigoriev, V. Fateev, A. Aukauloo and C. Etiévant, *International Journal of Hydrogen Energy*, 2011, **36**, 4134–4142.

[6] C. Galeano, J. C. Meier, V. Peinecke, H. Bongard, I. Katsounaros, A. A. Topalov, A. Lu, K. J. J. Mayrhofer and F. Schüth, *Journal of the American Chemical Society*, 2012, **134**, 20457–20465.

[7] M. S. El-Deab and T. Ohsaka, *Electrochemistry Communications*, 2002, **4**, 288–292.

[8] B. K. Jena and C. R. Raj, *Langmuir*, 2007, **23**, 4064–4070.

[9] B. Wang, *Journal of Power Sources*, 2005, **152**, 1–15.

[10] F. W. Campbell and R. G. Compton, *Analytical and Bioanalytical Chemistry*, 2010, **396**, 241–259.

[11] C. R. Rao, G. U. Kulkarni, P. J. Thomas and P. P. Edwards, *Chemical Society Reviews*, 2000, **29**, 27–35.

[12] A. Lavacci, H. Miller and F. Vizza, *Nanotechnology in Electrocatalysis for Energy*, Springer, 2014.

[13] D. Uzio and G. Berhault, *Catalysis Reviews*, 2010, **52**, 106–131.

[14] R. J. White, R. Luque, V. L. Budarin, J. H. Clark and D. J. Macquarrie, *Chemical Society Reviews*, 2009, **38**, 481–494.

[15] W. Plieth, *Journal of Physical Chemistry*, 1982, **86**, 3166–3170.

[16] Y. Wang, K. R. Ward, E. Laborda, C. Salter, A. Crossley, R. M. Jacobs and R. G. Compton, *Small*, 2013, **9**, 478–486.

[17] Y. Wang, E. Laborda, K. R. Ward, K. Tschulik and R. G. Compton, *Nanoscale*, 2013, **5**, 9699–9708.

[18] Y. Wang, E. Laborda, B. J. Plowman, K. Tschulik, K. R. Ward, R. G. Palgrave, C. Damm and R. G. Compton, *Physical Chemistry Chemical Physics*, 2014, **16**, 3200–3208.

[19] M. Gara, K. R. Ward and R. G. Compton, *Nanoscale*, 2013, **5**, 7304–7311.

[20] K. R. Ward, M. Gara, N. S. Lawrence, R. S. Hartshorne and R. G. Compton, *Journal of Electroanalytical Chemistry*, 2013, **695**, 1–9.

[21] J. M. Kahk, N. V. Rees, J. Pillay, R. Tshikhudo, S. Vilakazi and R. G. Compton, *Nano Today*, 2012, **7**, 174–179.

[22] M.-C. Daniel and D. Astruc, *Chemical reviews*, 2004, **104**, 293–346.

[23] S. Raj, P. Rai and Y.-T. Yu, *Materials Letters*, 2014, **117**, 116–119.

[24] T. Teranishi, M. Hosoe, T. Tanaka and M. Miyake, *Journal of Physical Chemistry B*, 1999, **103**, 3818–3827.

[25] S. Raj, G. Adilbish, J.-W. Lee, S. Manohar Majhi, B.-S. Chon, C.-H. Lee, S.-H. Jeon and Y.-T. Yu, *Ceramics International*, 2014, **40**, 13621–13626.

[26] M. Giersig and P. Mulvaney, *Langmuir*, 1993, **9**, 3408–3413.

[27] C. C. M. Neumann, C. Batchelor-McAuley, K. Tschulik, H. S. Toh, P. Shumbula, J. Pillay, R. Tshikhudo and R. G. Compton, *ChemElectroChem*, 2014, **1**, 87–89.

[28] K. Tschulik, C. Batchelor-McAuley, H.-S. Toh, E. J. Stuart and R. G. Compton, *Physical Chemistry Chemical Physics*, 2014, **16**, 616–623.

[29] K. R. Ward, N. S. Lawrence, R. S. Hartshorne and R. G. Compton, *The Journal of Physical Chemistry C*, 2011, **115**, 11204–11215.

[30] Y. Wang, E. Laborda, C. Salter, A. Crossley and R. G. Compton, *Analyst*, 2012, **137**, 4693–4697.

[31] M. O. Finot, G. D. Braybrook and M. T. McDermott, *Journal of Electroanalytical Chemistry*, 1999, **466**, 234–241.

[32] A. Kolics, A. E. Thomas and A. Wieckowski, *Journal of the Chemical Society, Faraday Transactions*, 1996, **92**, 3727–3736.

[33] Y.-G. Zhou, N. V. Rees, J. Pillay, R. Tshikhudo, S. Vilakazi and R. G. Compton, *Chemical Communications*, 2011, **48**, 224–226.

[34] R. G. Compton and C. E. Banks, *Understanding Voltammetry, 2nd ed.*, Imperial College Press, 2011.

[35] V. Andoralov, M. Tarasevich and O. Tripachev, *Russian Journal of Electrochemistry*, 2011, **47**, 1327–1336.

[36] C. M. Sánchez-Sánchez and A. J. Bard, *Analytical Chemistry*, 2009, **81**, 8094–8100.

[37] P. Quaino, N. Luque, R. Nazmutdinov, E. Santos and W. Schmickler, *Angewandte Chemie International Edition*, 2012, **51**, 12997–13000.

[38] E. Yeager, *Electrochimica Acta*, 1984, **29**, 1527–1537.

[39] V. Viswanathan, H. A. Hansen, J. Rossmeisl and J. K. Nørskov, *ACS Catalysis*, 2012, **2**, 1654–1660.

[40] D. Morales-Acosta, D. L. De La Fuente, L. Arriaga, G. V. Gutiérrez and F. Varela, *International Journal of Electrochemical Science*, 2011, **6**, 1835–1854.

[41] G. Brug, M. Sluyters-Rehbach, J. Sluyters and A. Hemelin, *Journal of Electroanalytical Chemistry and Interfacial Electrochemistry*, 1984, **181**, 245–266.

[42] B. E. Hayden, *Accounts of Chemical Research*, 2013, **46**, 1858–1866.

[43] A. S. Bandarenka and M. T. M. Koper, *Journal of Catalysis*, 2013, **308**, 11–24.

[44] L. Ly, C. Batchelor-McAuley, K. Tschulik, E. Kätelhön and R. Compton, submitted.